Accepted Manuscript

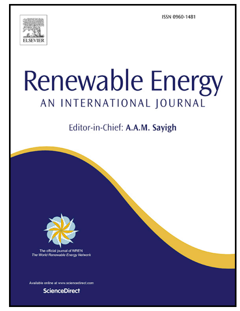

Description and performance analysis of a flexible photovoltaic/thermal (PV/T) solar system

Antonio Gagliano, Giuseppe M. Tina, Francesco Nocera, Alfio Dario Grasso, Stefano Aneli

PII: S0960-1481(18)30465-8

DOI: 10.1016/j.renene.2018.04.057

Reference: RENE 10015

To appear in: *Renewable Energy*

Received Date: 10 August 2017

Revised Date: 4 April 2018

Accepted Date: 16 April 2018

Please cite this article as: Gagliano A, Tina GM, Nocera F, Grasso AD, Aneli S, Description and performance analysis of a flexible photovoltaic/thermal (PV/T) solar system, *Renewable Energy* (2018), doi: 10.1016/j.renene.2018.04.057.

Description and performance analysis of a flexible Photovoltaic/Thermal (PV/T) solar system

Antonio Gagliano[a], Giuseppe M. Tina[a*], Francesco Nocera[a], Alfio Dario Grasso[a], Stefano Aneli[a]

[a] University of Catania, Electric, Electronics and Computer Engineering Department, V.le A.Doria n.5 , 95125 Catania, Italy

Abstract The main objectives of the present paper are to describe a pilot cogenerative PV/T plant and discuss its preliminary electrical and thermal experimental data. The PV/T plant is installed in the campus of the University of Catania, (Catania, Italy) on the eastern coast of Sicily, right in the centre of the Mediterranean area. The operative conditions of the experimental PV/T plant can be modified to implement parallel and series electrical and hydronic connections to the PV/T modules. The electrical and thermal load supplied by the PV/T plant can also be managed in order to simulate different energy demand scenarios. This study reports the main thermal and electrical operating parameters of the PV/T plant on the basis of experimental measurements, with the PV/T modules connected in series. A good level of correspondence was found between the measurements and the simulations obtained from a model of the system, particularly as regards electrical features.

Keywords: solar energy; photovoltaic/thermal system; modelling; experimental tests.

1. Introduction

In the few last years, the development of solar power systems has been led by the Photovoltaic (PV) technology, which is experiencing rapid, solid growth. Indeed, in 2016 global installed PV capacity reached a peak of over than 300 GW, corresponding to annual energy output of 365-TWh. At present, PV technology is used worldwide: in 2016, 24 countries exceeded the 1-GW power level, six countries reached more than 10 GW of total capacity, four attained more than 40 GW (Japan 42.8 GW, Germany 41.2 GW, USA 40.3 GW) and China alone reached 78 GW [1]. The Si-wafer based PV technology accounted for about 93% of total output in 2015. Multi-crystalline technology now generates about 68% of total output. In the last 10 years, the average efficiency of commercial wafer-based silicon modules has increased from about 12% to 17%. At the same time, CdTe module efficiency has increased from 9% to 16% [2]. This means that only less than 20% of solar energy can be converted into electricity, while more than 50% of incident solar radiation is dissipated as heat. Moreover, the main source of energy losses for a PV plant is the high operating temperature of PV cells (shading losses are not considered as they are almost exclusively dependent on array design and the presence of obstacles [3]).

Obviously, module electrical efficiency can be improved by removing the excess heat using active or passive cooling systems [4]. This latter consideration, together with the reduction in the number of useful surfaces available for installation of solar thermal systems due to the widespread adoption of small and medium size PV plants on the roofs of buildings (), has renewed interest in hybrid Photovoltaic/Thermal (PV/T) collectors. Recent review papers [5,6] have provided a systematic analysis of the historical and recent trend in PV/T technology, highlighting the performance and economic feasibility of PV/T systems using different heat transfer fluids and designs and for different application areas.

A large number of theoretical and experimental studies on PV/T collectors and systems have also been reported in the literature. The first study on a PV/T system was presented by Wolf in 1976 [7].

In 2001, Kalogirou [8] simulated a hybrid photovoltaic–thermal plant installed in Cyprus using TRNSYS. The results demonstrated that the hybrid system can increase the mean annual efficiency of the PV solar system from 2.8% to 7.7%. In addition, the PV/T plant can cover up to 49% of a house's hot water needs, thus increasing the system's mean annual efficiency to 31.7%.

In 2005, M. Bakker et al. [9] simulated PV/T collectors and a ground coupled heat pump in TRNSYS 25-m2. The results showed that their system was able to meet 100% of the total heat demand for a typical newly-built one-family dwelling, while covering nearly all its electric energy demand and keeping the long-term average ground temperature constant.

In meantime, Notton et al. [10] have developed a finite-differences simulation model. This model was validated using experimental data and let to estimate the cell temperature with a root mean square error of 1.3 °C. The work was proposed as an alternative to TRNSYS in order to model new hybrid PV/T collectors and estimate their thermal and electrical performances.

In 2008, Dubey and Tiwari [11] designed one of the first integrated photovoltaic (glass-to-glass) thermal solar water heater systems and tested it in outdoor conditions in India. They also came up with an analytical expression for the characteristic equation of PV/T collectors, experimentally validated for evaluating system performance for various configurations.

Similarly, Erdil et al. [12] have designed and tested a hybrid PV/T system for energy collection in Cyprus, with water used as the cooling fluid. They reported that 2.8 kWh of thermal energy could be stored as pre-heated water for domestic utilization with 11.5% electrical energy loss.

In 2010, Corbin and Zhai [13] suggested a new application for PV/T systems. They proposed integrating PV/T systems into the building façade. These collectors were capable of providing hot water for domestic use or hydronic space heating with total efficiency of 34.9% and no additional roof space requirements.

In 2012, Huang et al [14] carried out an experimental study on a PV/T system composed of a 240-W poly-crystalline silicon collector, a 120-L storage tank and a pump. The results showed system thermal efficiency and photovoltaic conversion efficiency as high as 35.33% and 12.77%, respectively.

In meantime, Ozgoren et al. [15] studied a system made up of a 190-W PV module and a190-W PV/T commercial water collector linked to a 175-L storage tank. They experimentally measured a PV/T collector thermal efficiency of 51% and maximum electrical efficiency of 13.6% for a mass flow rate of 0.03 kg/s. The electrical efficiency fell to 8% when the PV module temperature was 65 °C. They also observed that for each 100-W/m2 increase in solar radiation value the cell temperature increased about 1.2 °C for the PV/T system and 5.4 °C for the PV system, respectively.

In 2014, Dupeyrat et al. [16] built a new prototype of a PV/T system that was tested under the same conditions and requirements for certification tests of thermal collectors. The parameters extracted from their tests were used in TRNSYS simulations. The results showed that a PV/T system on a limited roof area provides not only higher total PV and energy output but also higher primary energy saving than side-by-side installations with conventional ST and PV components. The increase in electrical output for the equivalent roof area for the PV/T/PV combination was around 12.7% in Paris, 12.6% in Lyon and 10.7% in Nice.

The research of Herrando et al. [17] tried to maximize the supply of both electricity and hot water in the scenario of an average 3-bedroom terraced house in London, UK, while also maximizing the total CO2 emission savings. They found out that with a completely covered collector and a flow-rate of 20 L/h, 51% of the total electricity demand and 36% of the total hot water demand over a year could be covered by a hybrid PV/T system with a saving of up to 16.0 tons of CO2. In addition, the electricity demand coverage was slightly higher than the PV-only system equivalent (49%).

In 2015, Huang and Hsu [18] investigated the performance of a PV/T system made up of six 240-W PV modules with copper pipes circulating water on the back of a 500-L water tank. Electrical efficiency was 13.26% and thermal efficiency 17.34% in the zero-reduction condition. The average performance ratio of the PV/T system was 86%.

Aste et al [19] developed a PV/T system simulation model and evaluated its accuracy by means of an experimental monitoring campaign on a prototype. The collector was installed at the Politecnico di Milano, Italy, experimental station, with tilt angle of 30° and azimuth equal to 0°. The 125-W unglazed PV/T collector was connected to an insulated 200-L storage tank. They measured thermal and electrical performance in December. They found a daily mean PV/T electrical efficiency of 6.0% and thermal energy efficiency of 25%.

Allan J et al. [20] developed a new methodology to characterize the performance of PV/T collectors using an indoor solar simulator. In particular, they studied different PV/T system configurations and, in agreement with other studies, they found that serpentine collectors have the highest combined efficiency in comparison with other configurations.

In 2017, Bianchini et al [21] started to monitor the potential of a commercial PV/T solar collector for supplying electricity and thermal energy for domestic hot water (DHW) production in central Italy (or central-southern Europe in general).

Ramos et al [22] started to assess the technical potential and basic economic implications of integrating PV/T systems in the domestic sector, specifically regarding the provision of combined heating, cooling and electricity. They proposed different solutions for 4–5 person households, with a 100 m2 floor area and 50 m2 rooftop area available for installation of solar collectors, in ten selected European locations with distinct climatic conditions, using annualized data of varying temporal resolution. They found out that the most efficient system configuration involves the coupling of PV/T to water-to-water heat pumps. In addition, TRNSYS analyses indicated that PV/T systems were capable of covering 60% of the combined heating demands and almost 100% of the cooling demands of the households examined in middle and low European latitude regions.

The studies reported in the literature have therefore shown that PVT/T systems offer some advantages as compared with PV or solar thermal systems alone.

However, the literature survey revealed that, although many studies have investigated the PV/T system, there are relatively few works based on experimental research [10, 12, 13, 14, 15, 19, 21, 22, 23, 24, 25]. In particular, only two of these studies [14, 24] refer to unglazed PV/T systems.

The present study investigates the performance of a pilot plant constructed using unglazed PV/T panels installed in the campus of the University of Catania (Catania, Italy).

Therefore, since the existing experimental studies [14] and [19] were performed in Taiwan and Milan respectively, one of the novelties of this research is the study of an unglazed PV/T system in a typical Mediterranean climate. Moreover, the PV/T modules used are not thermally insulated.

This characteristic should allow the achievement of a good compromise between the thermal and electrical performances of PV/T panels in a mild climate. This means accepting higher heat losses in winter and lower PV cell temperatures in summer.

Therefore, we believe that this study could help to increase knowledge of the performances of unglazed, uninsulated PV/T plants in the Mediterranean area.

With the aim of enriching the state of the art of PV/T systems, this paper reports the implementation, simulation and preliminary experimental validation of a pilot water-cooled PV/T plant. The system is described from a hardware point of view, providing details on both the hydronic and the electrical sections. The software adopted to monitor and control the plant is also described. The system was modelled using TRNSYS and simulation results were compared with the experimental data collected during a one-week period.

The preliminary results indicate that the model developed in TRNSYS is quite reliable for simulating the behaviour of a PV/T system in the climatic conditions and with the design solutions used in this study.

2. PV/T solar plant description

One of the distinctive features of the proposed PV/T system is its high degree of flexibility, allowing simultaneous management of both the electrical and the thermal load to emulate different energy demand scenarios. Moreover, it is possible to switch the collectors' electrical and hydronic connections in order modify the plant's operative conditions from parallel to series connection of the PV/T modules in terms of both subsystems.

In a PV/T plant, the hybrid modules constitute the connection point between the electrical and the hydronic subsystems.

The PV/T solar plant consists of two Dualsun™ (France) modules. Table 1 contains the main geometric, electric and thermal characteristics of the modules defined according to EN 12975-1:2006 test methods.

Table 1: technical characteristics of the PV/T module

General data			**Electrical data**		
Length	1667	mm	Number of cells	60	
Width	990	mm	Cell type (dimensions)	Monocrystalline (156mm x 156mm)	
Frame thickness	40	mm	Nominal power, P_{MPP}	250	Wp
Weight whenempty/filled	30/31.7	Kg	Module efficiency,	15.4	%
Thermal data			Power tolerance	±3	%
Gross area	1.66	m^2	Rated voltage, V_{MPP}	30.7	V
Aperture area	1.6	m^2	Rated current, I_{MPP}	8.15	A
Heat transfer liquid vol.	1.7	l	Open circuit voltage, V_{oc}	38.5	V
Heat transfer liquid	water		Short circuit current, I_{sc}	8.55	A
Maximum temp.	74.7	°C	Maximum system voltage	1000	V
Max. operating pressure	1.2	Bar	Reverse current load	15	A
Pressure loss per module	6000 Pa at 200 l/h		NOCT	49	°C
Water inlet/outlet	15/21	mm	Connectors	MC4PLUS	
Thermal efficiency			Application class	Class A	
Optical efficiency a_0	55	%	Thermal coeff. V_{oc}	-0.32	%/K
heat loss coefficient a_1	15.76	$W/K/m^2$	Thermal coeff. I_{sc}	0.048	%/K
heat loss coefficient a_2	0	$W/K^2/m^2$	Efficiency loss with temperature	-0.44	%/°C

Thermal energy is transferred to the fluid by means of a rigid ultra-thin heat exchanger, completely integrated into the collector, which governs the heat transfer between the PV/T module front side and the fluid circulating on the back side.

The modules are installed on the roof of building 13 of the University Campus of Catania (Lat. 37.5256 N, Long. 15.0746 E), with a tilt angle β = 25° and azimuth angle γ=0° (South-facing). The tilt angle can be changed manually from 15° to 60°, with an angle step, $\Delta\beta$, equal to 5°. Fig.1 shows the deployed PV/T array and a detail of the structure allowing to modification of the tilt angle.

Fig. 1. Mounting structure: a) PV/T modules – b) Tilt angle setting structure, β.

The outline of the thermal section of the PV/T solar plant is shown in Fig. 2. The main components of the hydronic circuit are: two PV/T modules; one solar thermal tank with two heat exchangers; one water pump; ten temperature sensors; four flow meters (although in case of series connection only two are used); one data acquisition system; safety components; water shut-off valves; three-way valves; one dry cooler. The function of the dry cooler loop, or secondary circuit, is to emulate the energy demand for domestic hot water production.

The PV/T hydronic system designed allows series or parallel connection of the two modules, which can be selected by means of flow divider valves. The capability for modifying the configuration of the PV/T plant has a dual purpose: to test the operation of the two modules subjected to different conditions of shading (parallel connection) and to evaluate the variation of the electrical efficiency due to non-uniform temperature between the modules (series connection).

Three-way valves manage the flow rates circulating in the two modules with the aim of controlling their operating temperatures in accordance with weather conditions (irradiance, ambient temperature, wind speed) and thermal energy demand.

The hydronic circuit variables measured are: inlet and outlet temperatures of the operative fluid (water) at the inlet and outlet of each module, namely $TM_{i,in}$ and $TM_{i,out}$, at the inlet and outlet of the thermal solar tank, $T_{ST,in}$ and $T_{ST,out}$, at the bottom and in the top of the solar tank, $T_{ST,up}$ and $T_{ST,dw}$, as well as the fluid volumetric flowrate, m_s. The temperatures, T_{Cout} and T_{Cin}, and cooling volumetric flowrate, m_c, are also measured in the cooling circuit. The temperatures in the back of the modules ($T_{M1,b}$ and $T_{M2,b}$) are measured as well.

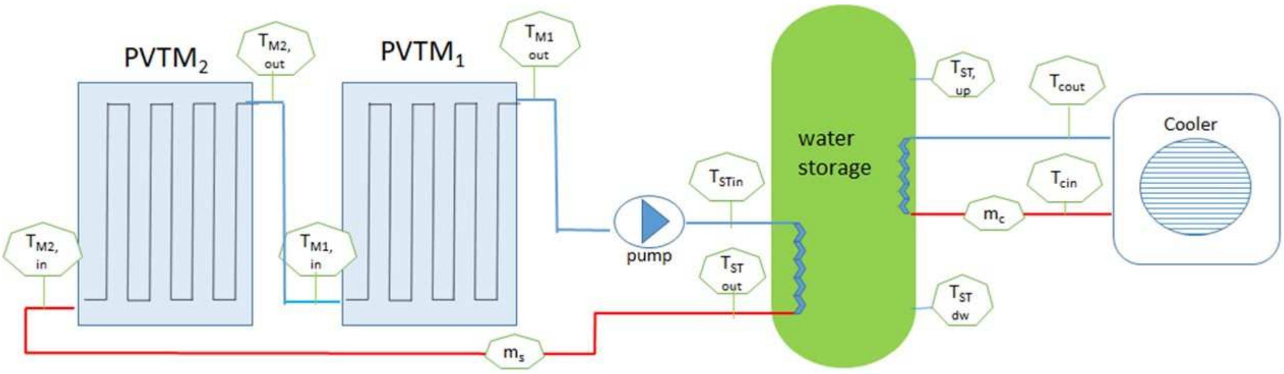

Fig. 2. Diagram of the hydronic section of the PV/T plant with the measured variables.

Table 2 contains the main characteristics of the hydronic circuit. Fig. 3 shows the installed hydronic section of the PV/T plant.

Table 2 – main characteristics of the hydronic circuit.

Pump		**Solar Thermal tank**		**Cooling device**	**Pipes**	
Maximum flow rate	Power	water tank	Water thermal capacity	Nominal power	Pipe length	Pipe diameter
55 l/min	3-45 W	0.185 m^3	4.174 (kJ/kg.K)	5000 W	40 m	16 mm

Fig. 3. View of the hydronic section of the PV/T plant.

Fig. 4 shows a close-up of the power and measurement boxes. The switchboard contains the main switches which supply power to the solenoid valve, the cooling circuit, the pump and all the components for control of the whole system. A remote-controlled relay card is used to manage the three-way valves. The data acquisition units (DAQ) are installed in the box on the right and acquire the analogic and digital signals measured on the PV/T plant and send them to a PC with a Supervisory Control and Data Acquisition (SCADA) system, as detailed in Section 5.

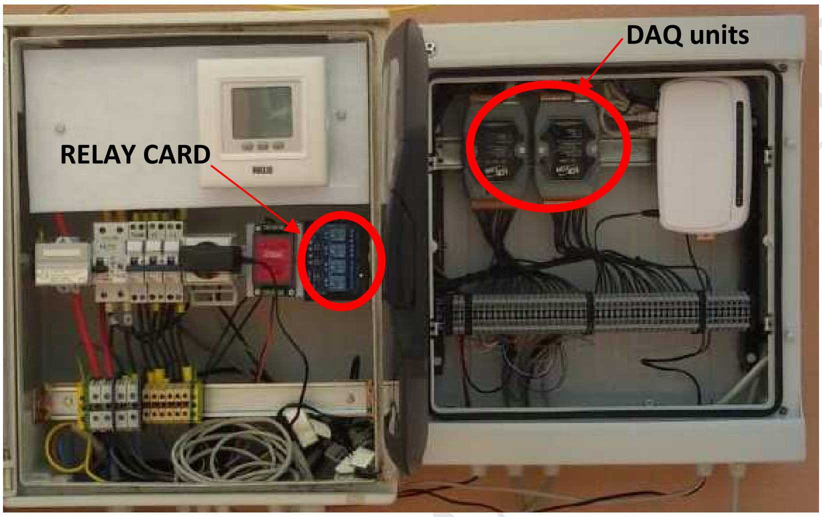

Fig. 4. PV/T plant power and measurement boxes.

The Hydronic circuit is managed using the strategy commonly adopted to control conventional solar thermal systems, based on monitoring of the temperature in the solar thermal tank. The primary circuit pump is turned on when T_{M1out} is 5-°C higher than the temperature in the lower part of the solar thermal tank, and is switched off when $T_{ST,dw}$-T_{M1out} is lower than 2°C. Finally, when the temperature inside the solar thermal tank reaches a given set-up value, the dry cooler is turned on.
Environmental data, such as global and diffuse solar radiation, wind speed and direction, ambient temperature, humidity and air pressure, are measured by a weather station placed close to the PV/T modules. All the sensors are connected to the control unit, placed in an external box, which transfers the sensor data to the PC through Ethernet [26]. Data from the PV/T solar plant and local weather station are stored in a dedicated SCADA with 1 min. acquisition rate. A web page was created to allow the users to remotely monitor or set the parameters governing the PV/T plant, as detailed in Section 5.
Therefore, the plant described is an effective research tool, allowing the study of PV/T systems with different configurations and different application scenarios.

3. Hardware and software setup for electrical performance analysis

The main electrical characteristics of the PV/T modules, measured by the manufacturer in Standard Test Conditions (STC) and of the string, with modules series or parallel connected, are contained in Table 3.

Table 3 – Module electrical values (measured at STC conditions) in series and parallel configuration.

	Isc (A)	Voc(V)	Impp (A)	Vmmp (V)	Pp (W)
module M_1	8.664	38.645	8.089	31.376	253.813
module M_2	8.654	38.607	8.103	31.545	255.597
Series	8.55	77	8.15	61.4	500
Parallel	17.1	38.5	16.3	30.7	500

As already mentioned, the PV/T modules can be connected both in series and in parallel. Fig. 5 shows the wiring diagram of the PV/T electrical circuit in series configuration. The connectors of the PV/T string, or of just one module, and the sensor cable, are connected to two separate sections of the switchboard installed on the roof (QBTP). Then the cables leaving QBTP are connected to another switchboard (QBTS), containing the electrical switching and power distribution gear. The two connectors of the PV/T string are coupled to an Agilent N3300A programmable electronic load (EL).

The EL is connected by means of a GPIB cable/card to a Personal Computer (PC). The PC is programmed with a tool developed in Labview® environment allowing the EL to be controlled in a way that sets a specific operating point for the photovoltaic string. Three different electrical operating modes can be selected: 1) open circuit, 2) I-V curve and 3) Maximum Power Point Tracking (MPPT). This program also controls the electrical output of the modules.

Moreover, the measured irradiance on the plane of the PV/T modules, G, and the two back side temperatures, $T_{M1,b}$ and $T_{M2,b}$ are conveyed to the NI cDAQ 9188, so these data are also shown in real time by means of the Labview® program developed.

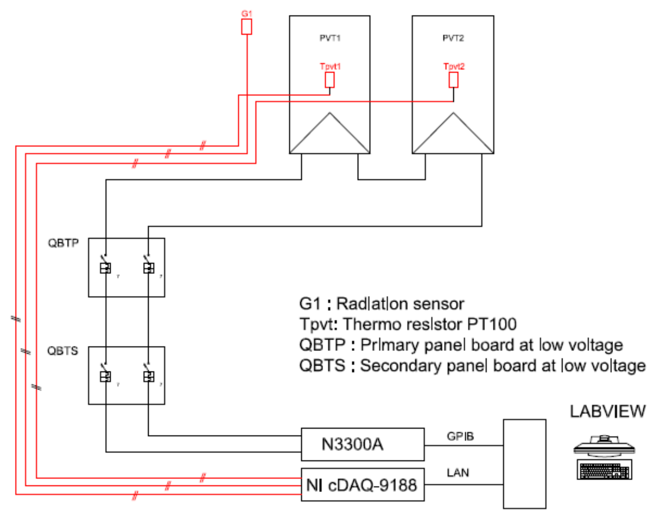

Fig. 5. PV/T system wiring diagram.

Selection of one of the different operating modes available allows the performance of experimental tests to evaluate the impact of the electrical operating point on the module working temperatures. For standard PV modules, it was evaluated that PV module temperatures can vary by up to 5°C in response to the switch from the no-load to the maximum power condition [27, 28]. PV module temperature is therefore a crucial parameter for optimal management of the PV/T system.

4. Model of the PV/T system in TRNSYS

A numerical study was developed using the TRNSYS 17 software in order to evaluate the thermal and electrical energy, the relative efficiencies and the transient behaviour of the PV/T plant.
As shown in fig. 6, the system consists of two main circuits:

a) solar loop (PV/T systems with a hot water storage tank)
b) cooling circuit (including storage and energy demand).

The TRNSYS user interface allows the connection of single components (called types) available in the program library, e.g. solar collector, pump, controller, heat exchanger. The model developed in TRNSYS mainly consist of the type shown in Table 4. TRNSYS solves the set of algebraic or differential equations that govern the different components with a user-selectable time step.

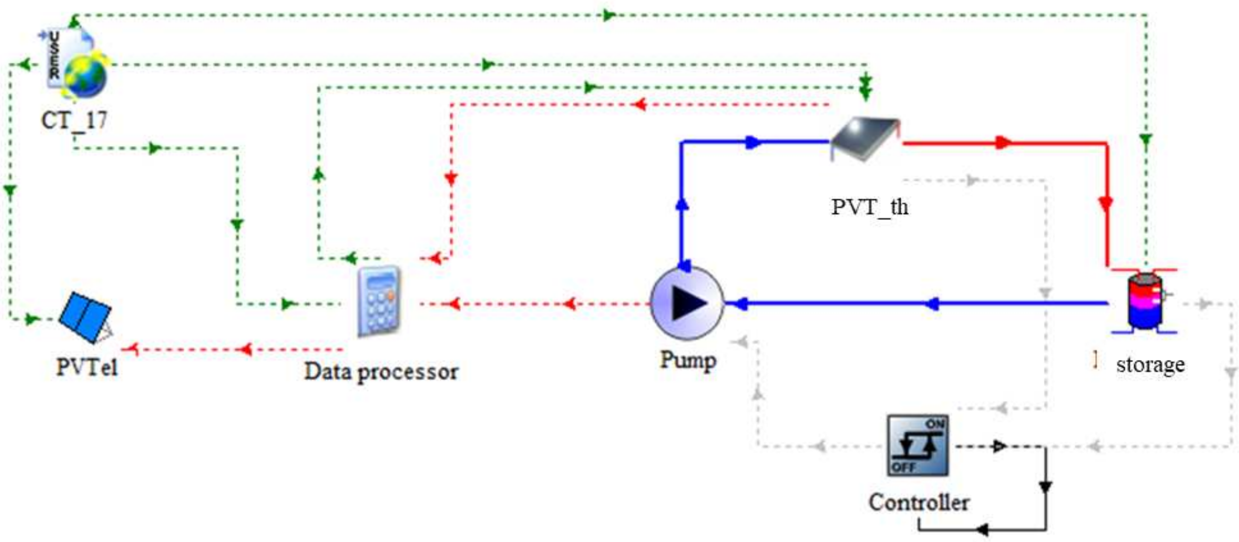

Fig. 6. Model of the PV/T plant

Table 4: Type used for the PV/T modelling

Type	109	1b	94a	3d	60d	2b	92	24
Name	Weather data	Solar collector	PV module	Pump	Storage Tank	Controller	Cooling circuit	Integral operator

The mathematical description of each type can be found in the TRNSYS manuals.
One peculiarity of this PV/T model is the approach used for defining the features of the PV/T module.
The type available in the TRNSYS library (type 50), needs values of τ, α, U_L and F ' as input data to characterize the thermal performance the PV/T module.
Currently, some PV/T modules, such as Dualsun modules, are tested in accordance with UNI EN 12975, which provides values of η0, a1 and a2. This hitch could be overcome converting data based on one standard (η_0, a_1 and a_2) with another (based on τ, α, U_L and F ') [solar collecting testing], or by fitting available experimental data.

However, even if such a procedure is feasible it could be subject to some inaccuracies compared to data obtained from laboratory tests.

Therefore, the PV/T module was defined using two distinct systems: one consisting of a solar thermal collector and the other of a photovoltaic module, operating in parallel. The performances of the thermal and photovoltaic modules were then evaluated, taking the mutual interference between the two systems into account.

This approach also allows use of the output of the photovoltaic type, i.e. current and voltage, for testing the plant's electrical performance.

It has to be pointed out that the approximation involved in the ways in which this study models two different components might lead to deviations between the experimental and the theoretical results.

As far as the photovoltaic system is concerned, the efficiency was calculated using the data provided by the producer and the temperature dependence of the photovoltaic cells, which in turn is coupled with the temperature of the thermal fluid (see eq. 7).

The efficiency of the thermal system was calculated with the aid of a simplified model using the modified solar radiation G_T [28]. G_T is calculated from the solar radiation “G” by subtracting the amount of solar energy converted by the photovoltaic effect (see eq. 3).

Weather data

The study was carried out using the weather data measured by the wheather station mentioned in Section 2, from 3 to 9 May, 2017. The data, originally collected in a Microsoft Office Excel® file, was converted into text format using a Matlab® script and then implemented within Type 109.

Solar collector (Type 1b)

The thermal efficiency of the solar thermal collector, η_{th}, was calculated through eq. 1 in steady-state conditions, while the thermal power is given in (2).

$$\eta_{th} = a_0 - a_1 \cdot \Delta T_m^+ - a_2 \cdot G_T \cdot \left(\Delta T_m^+\right)^2 \qquad (1)$$

$$P_{th} = A_{ST} - G_T \cdot \eta_{th} \qquad (2)$$

where

a_0=0.55, a_1 =15.76 W/(m^2 K),a_2 =0 W/(m^2 K^2) and ΔT^+m is the true mean fluid temperature difference [29]. G_T is the modified solar radiation calculated by subtracting from the solar radiation, G, the amount of solar energy converted by the photovoltaic effect, thus expressed by eq. 3,

$$G_T = G \cdot \left(1 - \eta_{el}\right) \qquad (3)$$

Assessment of the thermal efficiency in quasi-dynamic conditions also takes into account the wind effect and the thermal inertia of the PV/T solar system (ISO 9806:2013). However, for wind velocity lower than 4 m/s, the quasi-dynamic and steady-state models give comparable results for most collector designs.

In addition, the thermal power, P_{th}, produced by the PV/T solar plant in fig. 2 can be expressed as a function of the temperature difference between the water inlet and the outlet as

$$P_{th} = m \cdot C \cdot \left(T_{M1,out} - T_{M2,in}\right) \quad (4)$$

where m_s is the mass flowrate and C is the fluid specific heat.

PV module

In table 3 the electrical values of the PV modules are referred to STC (GSTC= 1000 W/m2 of global solar radiation PV module temperature of 25 °C). However, as we are all aware PV modules do not usually work at STC, and the electrical features provided in table 3 vary when they operate under different environmental conditions. Consequently, the actual DC power, P_{el}, differs from the nominal one, P_{nom}, due to variations in the module temperature, T_{PV}, and/or solar radiation, G. Therefore, the efficiency, η_{el}, is defined as the ratio between measured P_{el} and the product of the solar radiation G and the surface area of modules A_{PV}:

$$\eta_{el} = \frac{P_{el}}{A_{PV} \cdot G} \quad (5)$$

In the model designed, an external operator is introduced with the aim of calculating electrical efficiency as a function of module cell temperature, TPV (see eq. 6).
Module cell temperature is in turn defined as a function of the average of the inlet and outlet temperatures of the thermal fluid in the solar collector. The electrical efficiency is then calculated by

$$\eta_{el} = 0.154 \cdot \left[1 - 0.0044 \cdot \left(T_{PV} - 25\right)\right] \quad (6)$$

where T_{PV} is calculated as

$$T_{PV} = \frac{\left[\frac{\left(T_{M,in} + T_{M,out}\right)}{2} + T_a\right]}{2} \quad (7)$$

Equation 7 was derived by modifying the models available in the literature [30], which adopt the mean temperature of the cooling fluid, in accordance with results obtained from our experimental survey on this PV/T plant.

In order to evaluate the performance of the PV plant over time, IEC standard 61724:1998 introduces the array yield, Y_A, and the reference yield, Y_R. Y_A is defined as the ratio between the electrical energy produced in a defined time interval, E_{el}, and the nominal electrical power, P_{nom}. The array yield represents the number of hours in which the PV modules work at their peak value in the defined time interval:

$$Y_A = \frac{E_{el}}{P_{nom}} \quad (8)$$

Y_R is defined as the ratio between the solar radiation energy per surface unit, H, evaluated in the considered time interval and G_{STC}:

$$Y_R = \frac{H}{G_{STC}} \quad (9)$$

Finally, the performance ratio, PR, is defined as the ratio between the array yield Y_A and the reference yield Y_R:

$$PR = Y_A/Y_R \quad (10)$$

Therefore, PR provides the ratio between the nominal and actual efficiency of the PV plant.

Solar Storage Tank (Type 60d)

Type 60d allows modelling of a stratified cylindrical vertical storage tank with an inlet and an outlet flow rate and two internal heat exchangers (inlet 1 and 2). The heat exchanger, in the lower part of the solar storage tank, is connected with the solar collector circuit, while the heat exchanger, in the upper part of the storage tank, is connected with the auxiliary device. The inputs required are the flow rates at inlets 1 and 2 and the tank volume, which is 0.189 m^3. The average temperature of the tank is used as input for the ON/OFF controller that operates the pump. The type was set without considering thermal stratification.

Auxiliary cooling device (Type 92)

In this study, the auxiliary cooling device simulates DHW energy demand. The operating principle requires the cooling device to remove energy from the solar tank until a given temperature value (e.g., 40°C) is reached inside the solar tank. The thermal energy extracted by the solar tank is the useful thermal energy produced by the PV/T plant at the selected thermal level.

Integral Operator (Type 24)

The thermal energy transferred to the thermal storage E_{th} and the electricity produced,during the time period t_1-t_2, E_{el} are calculated by means of the integral operator,

$$E_{th} = \int_{t1}^{t2} \dot{m} \cdot C \cdot \Delta T \cdot dt \quad (11)$$

where:

$\dot{m}$ = water flow rate

$C = 4.186 \frac{kJ}{kg \cdot K}$

$\Delta T = \left(T_{ST\_in} - T_{ST\_out}\right)$

$$E_{el} = \int_{t1}^{t2} G \cdot A_{PV} \cdot \eta_{el} \cdot dt \quad (12)$$

5. Experimental results

The PV/T plant is monitored in real time by means of a dedicated SCADA system. The SCADA adopts low-cost commercial off-the-shelf sensors and components. The data acquisition board is the ICPDAS ET-7017 (20 analog single-ended channels with programmable input range). The information provided by the data acquisition board is acquired by a web-based application. The system can be interfaced to any device through the standard MODBUS TCP/IP protocol. The adoption of the TCP/IP version of MODBUS protocol allows the connection of a virtually unlimited number of masters and slaves over local networks and/or the World Wide Web. Among the main features, the software is capable of storing data from the individual sensors on a database; plotting stored data; viewing the captured data in real time; carrying out operations on aggregate data; generating periodic graphical and/or text file reports and sending them via e-mail; generating e-mail alerts and alarms and allowing remote access to the database via a web browser.

Fig. 7 shows a screenshot of the web page of the PV/T plant (accessible at http://moses.pvt.dieei.unict.it:8081), where the current configuration and the value of the operative variables (thermal, electrical and environmental) are reported in real time (inside the red boxes).

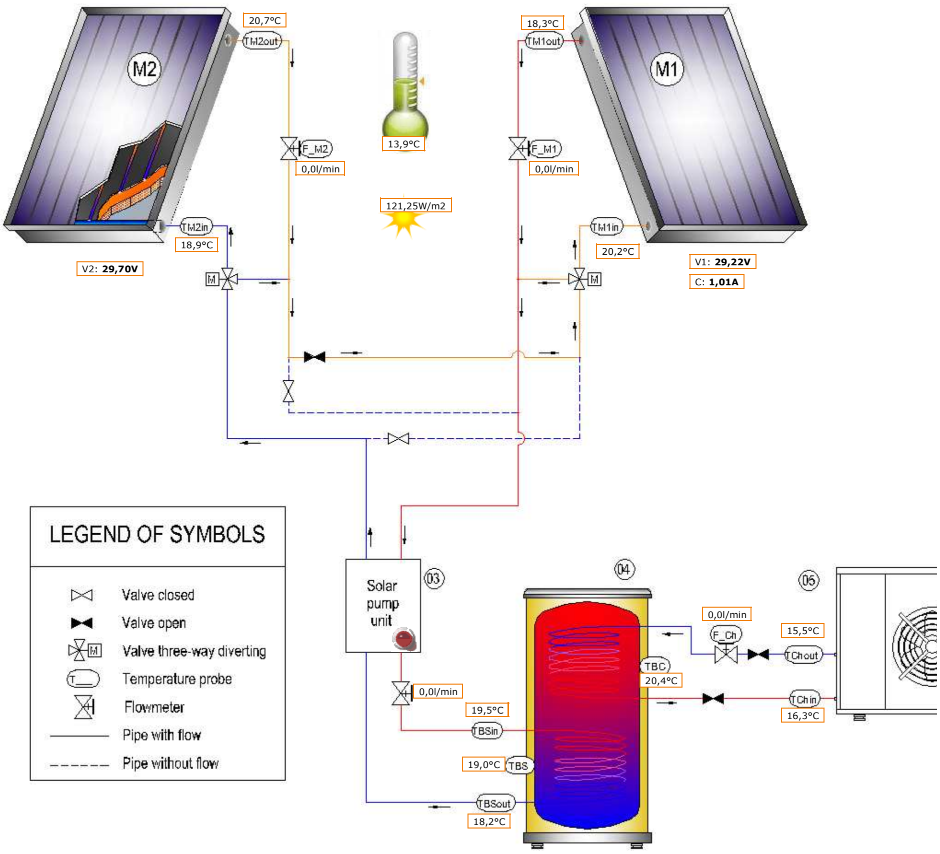

Fig. 7 Graphical view of the SCADA system

The architecture of the PV/T plant allows the temperature inside the storage tank to be managed by defining the temperature set-point that switches on the cooling device. Different scenarios of daily heat demand curves may be simulated by choosing the set points of the temperature inside the hot water storage tank [31]. Consequently, the global efficiency (thermal plus electrical efficiency) of the PV/T modules can be evaluated as a function of the different enthalpic level of the water in the solar tank. In fact, the global efficiency of a PV/T plant strongly depends on the operating temperatures. In other words, when the thermal level of the user demand is low, the PV module works at its maximum power point; in contrast, when the requested thermal level is high, electricity production is reduced due to the increase in PV cell temperature.

Below, the preliminary results obtained during a week of operation of the system in a single scenario are reported and discussed. The PV/T plant was set with the two modules connected in series, and the set-point temperature of 45°C in the upper part of the hot water storage tank (T_{ST_up}) had to be exceeded to switch on the cooling device.

Fig. 8 shows the plots of a week of measurements, from 3 to 9 May, 2017, of the following variables: irradiance on the plane of the modules (G); ambient temperature (T_{air}); temperature of the lower part of the storage tanks ($T_{ST,dw}$); and temperature at the outlet of module 1 ($T_{M1,out}$). In the period over 7-8 May there is an interruption in the recorded data due to a malfunction of a couple of thermal sensors.

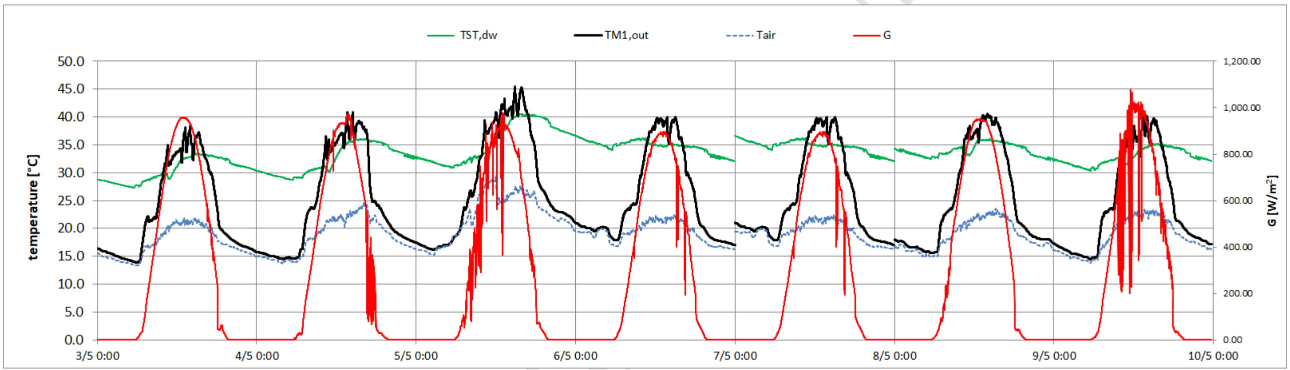

Fig. 8. Solar radiation (G), air temperature (T_{air}), M1 outlet temperature ($T_{M1,out}$), solar tank temperature (T_{ST_dw}),

During the monitored period, the temperature in the upper part of the hot water storage tank (T_{ST_up}) never exceeded 45°C, the temperature set point that activated the cooling device, so thermal energy was not extracted from the solar tank.

Regarding the electrical configuration, the two series-connected modules are operated at the maximum power point. The monitoring system acquires both the voltage and the current of each PV/T module, so the performances of the two modules are available separately.

Figs. 9 and 10 show the weekly variation of the electrical power ($P_{el,Mi}$) and the module back side temperature ($T_{Mi,b}$) of PV/T modules M2 and M1, respectively.

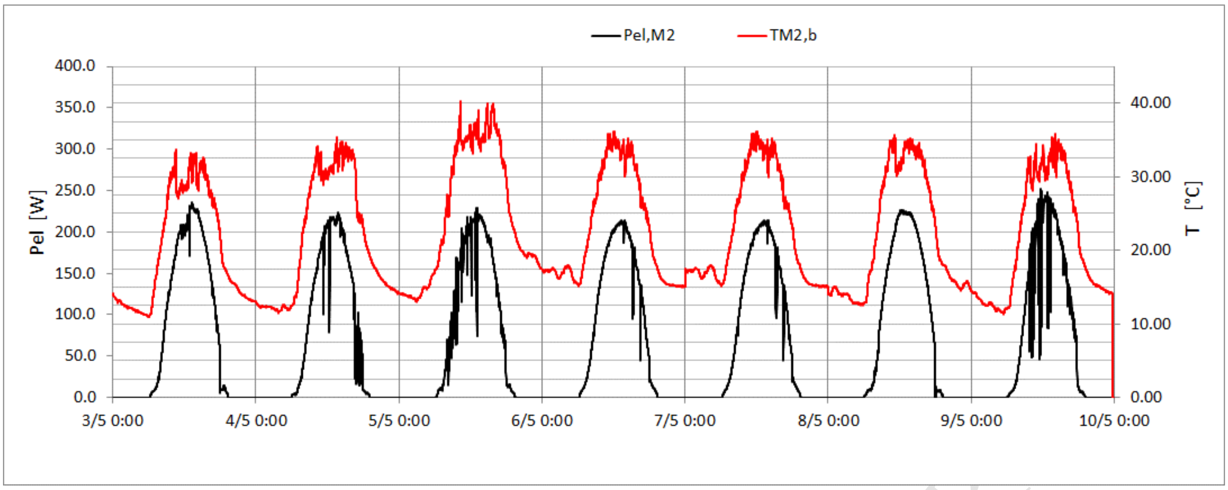

Fig. 9. Photovoltaic temperature and electrical power of PV/T module M2

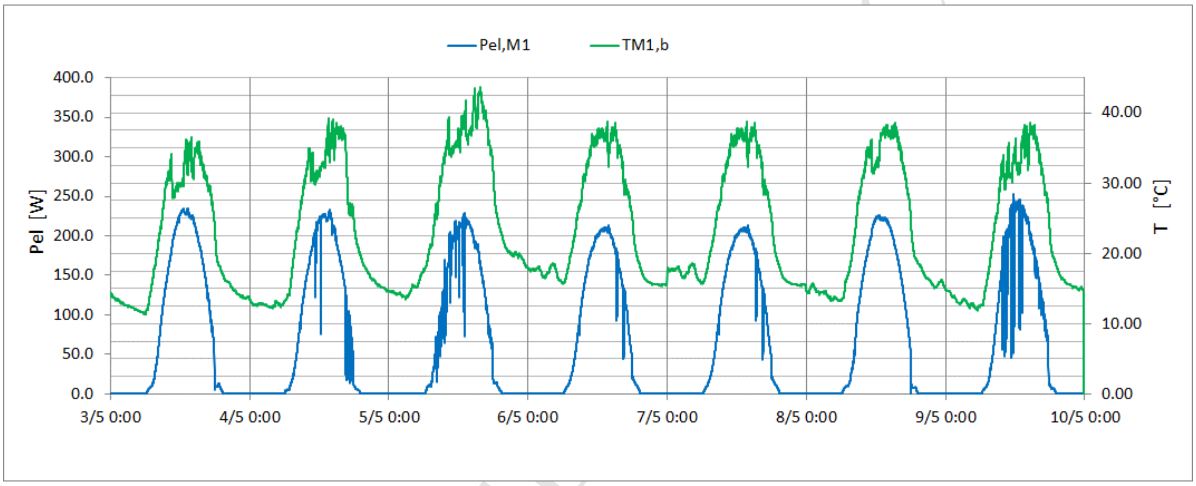

Fig 10. Photovoltaic temperature and electrical power of PV/T module M1

It can be seen that M2 has lower back side temperature than M1. This result is in agreement with the series-connection of the modules, which implies that the circulating fluid first enters M2 and then flows to M1. The maximum difference in the back temperatures is 3.0-4.0 °C, so the impact on the amount of electricity generated is quite low. Indeed, considering that the thermal power coefficient of the PV modules is -0.44%/°C (see Table 1), the increase in the electrical power generated is almost 1.5 %.

6. **Comparison with simulation results**

In this section the experimental data are compared with the results of the simulation performed using TRNSYS. This makes it possible to evaluate the accuracy of the model of the PV/T plant simulated in TRNSYS environment.
The percentage error between experimental and simulation data for some representative variables was calculated. The parameters considered were the thermal (ΔE_{th}) and electrical (ΔE_{ef}) energy produced by the PV/T plant, the outlet temperature ($\Delta T_{M1,out}$) and the voltage (ΔV_{M1}) of module 1. Table 5 shows the percentage error between simulated and experimental data.

Table 5: Percentage error between simulated and experimental data

	Min (%)	Mean (%)	Max (%)
$\Delta T_{M1,out}$	0.009	6.53	27.58
ΔV_{M1}	0.03	4.35	23.49
ΔE_{th}	2.22	12.04	28.31
ΔE_{el}	4.23	5.29	8.02

It can be seen that there is a wide range of variation in the percentage errors, with minimum values that are rather small, while the maximum values are rather high. Reflecting the complexity of the two sub-systems, the errors of the electrical parameters are lower than the errors observed for the thermal parameters. However, the mean errors may be acceptable considering the approximation affecting both the experimental and the simulation data.

The following figures depict the daily comparisons between the measured and simulated data. Fig. 11 compares the simulated and measured voltage of module M1. Module voltage is well known to be significantly affected by cell temperature, so this comparison allows assessment of the accuracy of the equation used for calculating T_{PV} (eq. 7). The two sets of data are in good agreement, especially during the central part of the day. However, the experimental values are significantly higher than the simulated ones in the early hours of the day, when the solar radiation is feeble. These discrepancies may be ascribed to inaccuracy of the MPPT algorithm at low solar radiation values. In these conditions, the module voltage tends to reach the open circuit voltage value (V_{oc}).

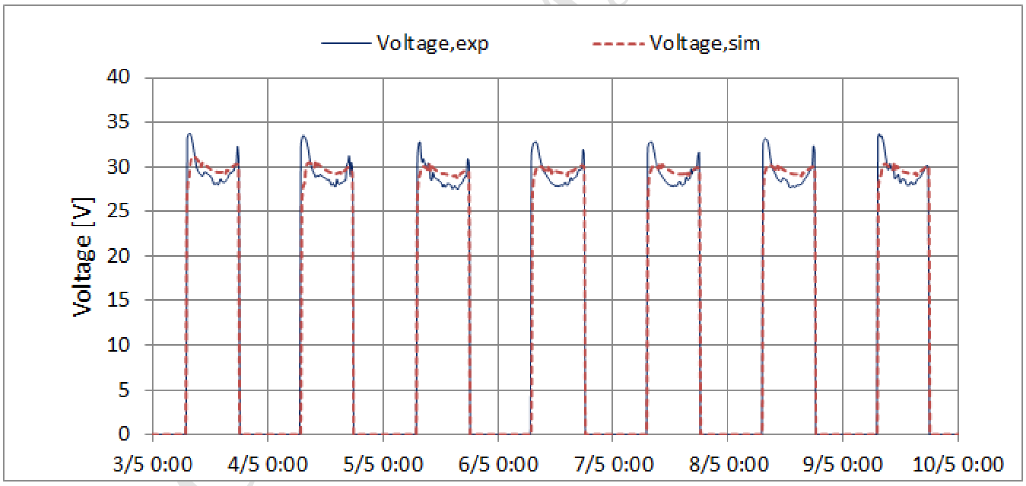

Fig. 11. Comparisons between simulated and measured voltage of PV/T module M1

Figs. 12 and 13 show the comparisons between electrical power (P_{el}) and electrical efficiency ($\eta_{,el}$). The modelled efficiency fits the experimental data quite well, whereas greater differences emerge between the two sets of electrical power values. This may be due to simplified model adopted for describing the electrical part of the PV/T module, since only thermal losses were considered, leaving aside other losses such as shading, soiling, optical losses, joule losses and MPPT losses.

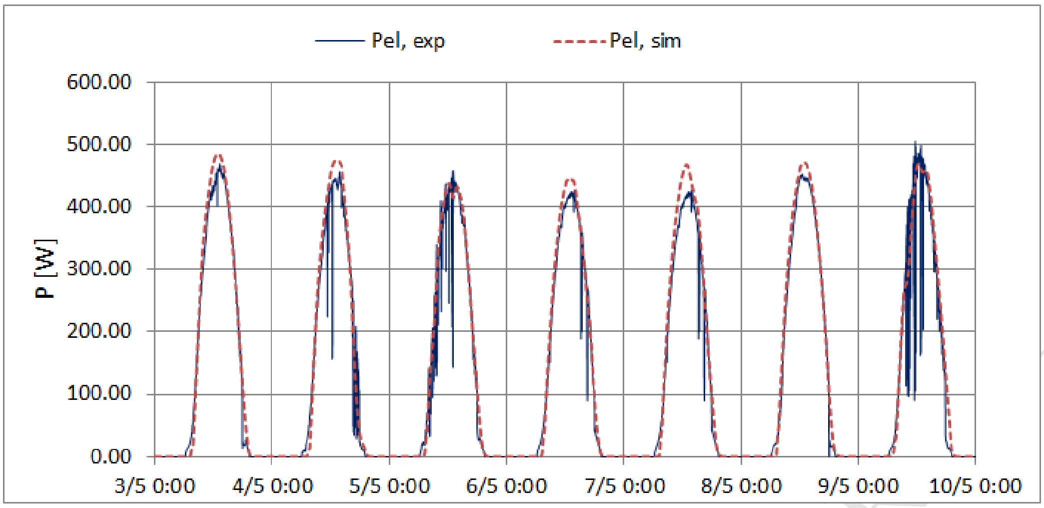

Fig. 12. Comparisons between experimental and simulated electric power (P_{el})

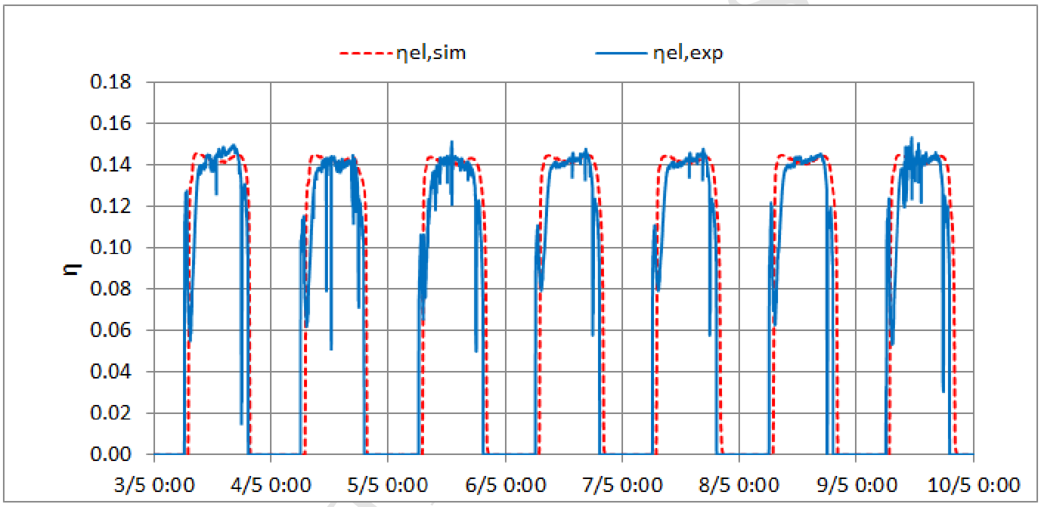

Fig. 13. Comparisons between experimental and simulated electric efficiency (η_{el})

As regards the thermal features, figure 14 displays the comparison between the measured temperature at the outlet of the PV/T module, T_{M1out_exp}, and the simulated value, T_{M1out_sim}, which are the highest hydronic circuit fluid temperatures.

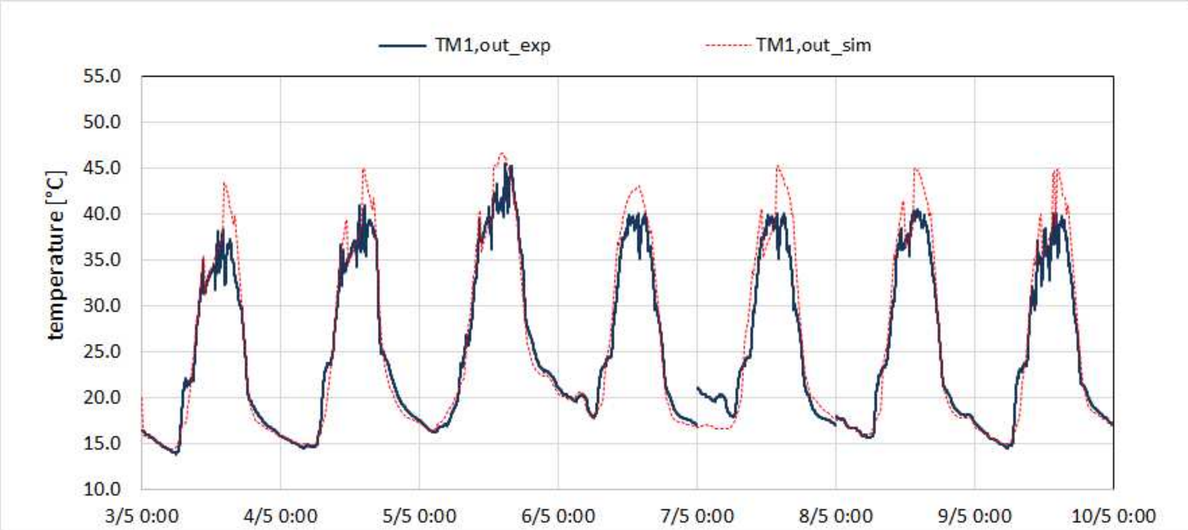

Fig. 14. Comparisons between experimental and simulated temperatures at the outlet of PV/T module M1

The trend of the two temperature sets is fairly comparable, with some significant differences during the second part of the day (after midday), when the increase in the temperature inside the solar tank causes the pump to stop. After this, it takes some time for the PV/T system to restart the pump, due to its inertia. In contrast, in the simulation, the modular outlet temperature rises rapidly and the pump restarts quickly. Obviously, it will be necessary to define a different control strategy to realign the model with the experimental plant.

Fig. 15 shows the comparison between the mean temperature measured inside the solar thermal tank, T_{ST_exp}, and the simulated value, T_{ST_sim}, where T_{ST_exp} is calculated by

$$T_{ST\_exp} = \frac{\left(T_{ST\_up} + T_{ST\_dw}\right)}{2} \tag{13}$$

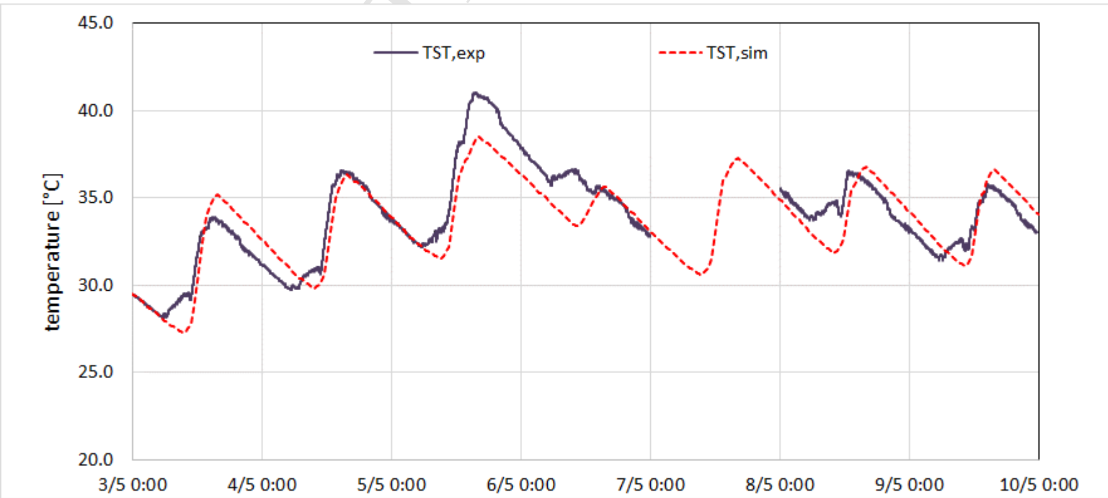

Fig. 15. Comparisons between experimental and simulated temperatures in the solar tank T_{ST}

Once again, the trends of the two temperature sets are fairly comparable. However, on some days obvious differences emerge between the experimental and simulated data, which may be partially attributed to the discrepancies in the module outlet temperature already highlighted. Moreover, temperature sensor measurement errors may play an important role. On 7 May, the experimental values of T_{ST} are not reported due to a fault in the temperature sensors.

Finally, the energy production of the PV/T plant is reported. Figure 16 displays the comparison of the daily thermal energies exchanged between the PV/T modules and the solar storage tank.

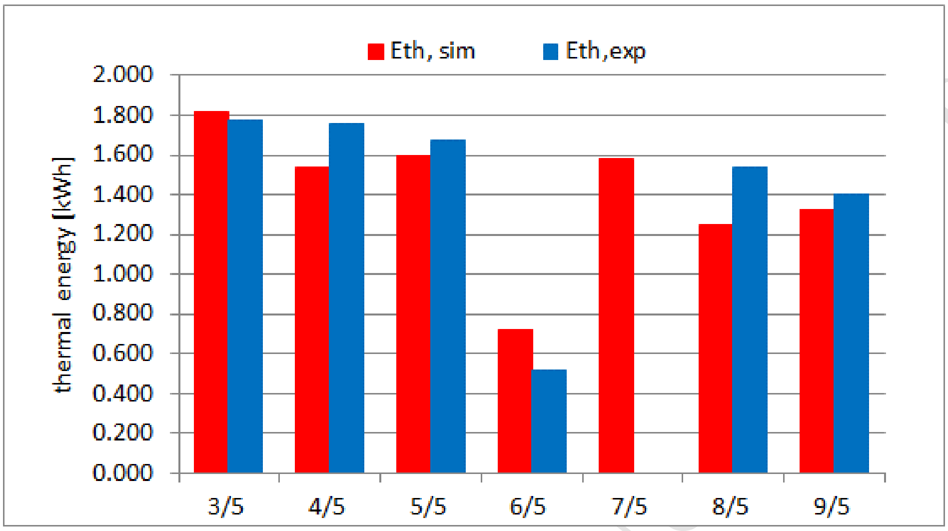

Fig. 16. Comparison of daily thermal energies: simulated ($E_{th,sim}$) and experimental ($E_{th,exp}$)

Overall, the matching between experimental and simulated data is good. On 6 May, the performance of the PV/T plant was poorer than on the other days. This is because the temperatures inside the solar tank are higher than the solar collector outlet temperatures. This condition turns off the pump and prevents the supply of energy to the solar tank.

Fig. 17 shows the daily values of the array yield, YA, reference yield, YR, and performance ratio, P_R, of the two modules.

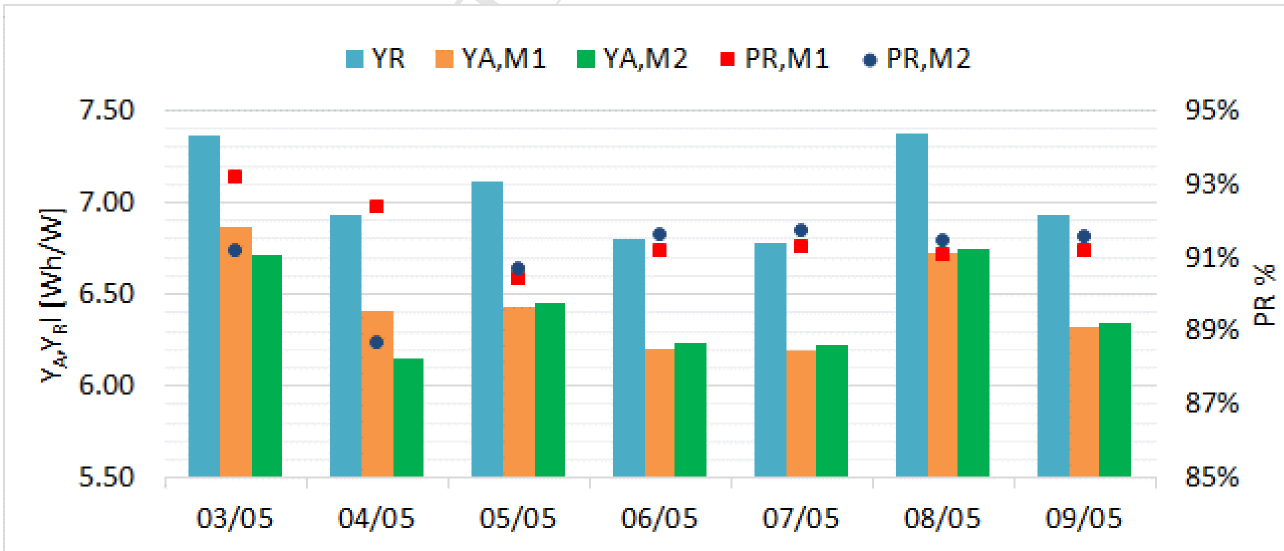

Fig. 17. Daily value of the array yield, YA, reference yield, YR and performance ratio (PR) of the two modules

PR is calculated as a function of both YA and YR by eq. 9-10. During the first two days, the hottest module M1 performed better, but this is due to a shading problem, since the difference in power is not justified by the difference in the TPV temperatures, whereas for the last five days the performances of the two modules are in accordance with the thermal analysis. It is worth noting that the PV/T modules always have a PR value higher than 88%, this means that the effective efficiency of the module is about 10% less than the nominal one. This result is comparable with that observed by [21].

7. Conclusions

This paper describes a pilot cogenerative PV/T plant installed in the campus of the University of Catania (Catania, Italy).

The energy demand may be varied through management of the cooler device and the electronic load (controlled and monitored by a specially developed software). This feature makes the system flexible in determining the electrical and thermal operating points of the PV/T modules. Although the PV/T plant is able to operate in both series and parallel configuration, this study only reports on preliminary tests conducted with the modules connected in series. The experimental survey provides useful data on the system's behavior and energy performances.

A TRNSYS model of the PV/T plant was also produced and the results of the simulations are reported. The comparison between the numerical data and the measurements is also presented. From this point of view, it was observed that the two sets of data are fairly comparable, with average errors of 12.04% and 5.29% respectively for the thermal and electrical energy produced by the system. Although the reported results are limited to a very short period, they provide some useful indications on the performances of a PV/T plant installed in the Mediterranean area.

The further development of this study is in the direction of extending the monitored period to one year, to obtain a complete analysis of the system also during the winter, and also to check the precision of the TRNSYS model in different weather conditions.

Acknowledgements

This research received a specific grant from the University of Catania: progetto di Ateneo, FIR 2014 (DC90C1): "L'integrazione degli impianti fotovoltaici e fotovoltaici/termici nei sistemi edilizi in area mediterranea: studio numerico e sperimentazioni sull'efficienza e sulla compatibilità costruttiva".

References

[1] 2016 - SNAPSHOT OF GLOBAL PHOTOVOLTAIC MARKETS, Report IEA PVPS T1-31:2017.

[2] PHOTOVOLTAICS REPORT, Fraunhofer Institute for Solar Energy Systems, ISE, 2016.

[3] G.M. Tina, Simulation Model of Photovoltaic and Photovoltaic/Thermal Module/String Under Nonuniform Distribution of Irradiance and Temperature. ASME. J. Sol. Energy Eng. 139 (2) (2016) 021013-021013-12. doi:10.1115/1.4035152.

[4] F.G. Cabo, S. Nizetic , G.M. Tina. Photovoltaic panels: a review of the cooling techniques. Trans FAMENA. 40 (2016) 63–74.

[5] A. H. A. Al-Waeli, K. Sopian, H.A. Kazem, M. T. Chaichan, PV/T (Photovoltaic/Thermal): Status and Future Prospects. Renewable and Sustainable Energy Review 77 (2017) 109-130.

[6] T. Brahim, A. Jemni, Economical assessment and applications of photovoltaic/thermal hybrid solar technology: A review. Solar Energy 153 (2017) 540-561. doi.org/10.1016/j.solener.2017.05.081
[7] M. Wolf, Performance analyses of combined heating and photovoltaic power systems for residences. Energy Convers 16(1-2) (1976) 79–90. doi.org/10.1016/0013-7480(76)90018-8
[8] S.A. Kalogirou, Use of TRNSYS for modelling and simulation of a hybrid pv-thermal solar system for Cyprus. Renew, Energy 23 (2001) 247-260. doi:10.1016/S0960-1481(00)00176-2
[9] M. Bakker, H.A. Zondag, M.J. Elswijk, K.J. Strootman, M.J.M. Jong, Performance and costs of a roof-sized PV/thermal array combined with a ground coupled heat pump. Sol. Energy 78 (2005) 331-339. doi:10.1016/j.solener.2004.09.019
[10] G.Notton, C.Cristofari, M.Mattei, P.Poggi, Modelling of a double-glass photovoltaic module using finite differences. Applied Thermal Engineering 25 (2005) 2854-2877. doi:10.1016/j.applthermaleng.2005.02.008
[11] Swapnil Dubey, G.N. Tiwari, Thermal modeling of a combined system of photovoltaic thermal (PV/T) solar water heater, Solar Energy 82(7) (2008) 602-612.
[12] E. Erdil, M. Ilkan, F. Egelioglu, An experimental study on energy generation with a photovoltaic (PV)-solar thermal hybrid system, Energy 33(8) (2008) 1241-1245. doi.org/10.1016/j.energy.2008.03.005.
[13] C.D. Corbin, Z.J. Zhai, Experimental and numerical investigation on thermal and electrical performance of a building integrated photovoltaic-thermal collector system, Energy Build. 42(1) (2010) 76-82. doi:10.1016/j.enbuild.2009.07.013.
[14] C.Y. Huang,, H.C. Sung, K.L. Yen Experimental Study of Photovoltaic/Thermal (PV/T) Hybrid System , International Journal of Smart Grid and Clean Energy 2(2) (2013) 148–151.
[15] M. Ozgoren, M. H. Aksoy, C. Bakir, S. Dogan Experimental Performance Investigation of Photovoltaic/Thermal (PV-T) System EPJ Web of Conferences 45 (2013). doi.org/10.1051/epjconf/20134501106
[16] P. Dupeyrat, C. Ménézo, S. Fortuin, Study of the thermal and electrical performances of PVT solar hot water system, Energy and Buildings 68(C) (2014)751-755. doi:10.1016/j.enbuild.2012.09.032
[17] M. Herrando, C. N. Markides, K. Hellgardt, A UK-based assessment of hybrid PV and solar-thermal systems for domestic heating and power: System performance, Applied Energy 122(1) (2014) 288-309. doi:10.1016/j.apenergy.2014.01.061
[18] C.-Y. Huang, K.-C. Hsu, Performance monitoring of photovoltaic thermal hybrid system The 14th IFToMM World Congress, Taipei, Taiwan, October 25-30, 2015
[19] N. Aste, F. Leonforte, C. Del Pero, Design, modelling and performance monitoring of a photovoltaic–thermal (PVT) water collector, Solar Energy 112 (2015) 85–99.
[20] J. Allan, Z. Dehouche, S. Stankovic, L. Mauricette, Performance testing of thermal and photovoltaic thermal solar collectors. Energy Science & Engineering, 3(4) (2015) 310-326. doi:10.1002/ese3.75
[21] A. Bianchini, A. Guzzini, M. Pellegrini, C. Saccani, Photovoltaic/thermal (PV/ T) solar system: experimental measurements, performance analysis and economic assessment, Renewable Energy. 111 (2017) 543-555
[22] A. Ramos, et al, Hybrid photovoltaic-thermal solar systems for combined heating, cooling and power provision in the urban environment, Energy Convers. Manag., 150 (2017) 838-850.
[23] T.T. Chow, W. He, J. Ji, An experimental study of facade-integrated photovoltaic/water-heating system, Applied Thermal Engineering, 27, 2007, 37-45.
[24] N. Aste, C. Del Pero, F. Leonforte, M. Manfren, Performance monitoring and modelling of an uncovered photovoltaic-thermal (PVT) water collector, Solar Energy, 135, 2016 551–568.
[25] N. Aste, G. Chiesa F. Verri, Design, development and performance monitoring of a photovoltaic-thermal (PVT) air collector, Renewable Energy Volume 33, Issue 5, May 2008, Pages 914-927.
[26] G. M. Tina, A.D. Grasso, A. Gagliano, Monitoring of solar cogenerative PVT power plants: Overview and a practical example. Sustain. Energy Technol. Assess. 10 (2015) 90–101.
[27] G.M. Tina, A coupled electrical and thermal model for photovoltaic modules, Journal of Solar Energy Engineering, 132 (2010) 1-5. doi: 10.1115/1.4001149.
[28] L.W. Florschuet, Extension of the Hottel- Whillier model to the analysis of combined photovoltaic/thermal flat plate collectors, Solar Energy, 22, 1979 361-36. doi: 10.1016/0038-092X(79)90190-7.
[29] Duffie JA, et al. Solar Engineering of Thermal Processes. John Wiley & Sons, 1974. ISBN: 0-471-22371-9
[30] S.A. Kalogirou, Y. Tripanagnostopoulos, Hybrid PV/T solar systems for domestic hot water and electricity production, Energy Conversion and Management, 47, 2006, 3368-3382.
[31] G Tina, A Gagliano, F Nocera, A Grasso, The Pilot Photovoltaic/Thermal Plant at the University of Catania: description and preliminary characterization, BIRES 2017, Dublin, Ireland.

Nomenclature

A_{PV} = area of the PV modules (m^2)
A_{ST} = area of the solar thermal absorber (m^2)
a_0 = ratio between the thermal power produced and a given solar radiation when there are not heat losses
a_1 = linear coefficient of thermal dispersion,
a_2 = quadratic coefficient of thermal dispersion ,
C = specific heat (kJ/kg°C)
E_{el} = electrical energy (kWh)
E_{th} = thermal energy (kWh)
G= solar irradiation (W/m^2)
G_{STC}= solar irradiation at STC (W/m^2)
G_T = modified solar radiation (W/m^2)
H = Solar Radiation (kWh/m^2)
k_θ = Incident Angle Modifier (IAM)
$\dot{m}_c$ = mass flow rate of cooler circuit (kg/s)
$\dot{m}_s$ = mass flow rate of solar circuit (kg/s)
P_{nom} = nominal electrical power (kW)
P_{PV} = electrical power (kW)
P_{th} = thermal power (kW)
T_{air} = outdoor temperature (°C)
$T_{c,in}$ = water temperature at the inlet of cooling circuit (°C)
$T_{c,out}$ = water temperature at the outlet of cooling circuit (°C)
$T_{Mi,in}$ = water temperature at the inlet of PV/T module "i" (°C)
$T_{Mi,out}$ = water temperature at the outlet of PV/T module "i" (°C)
$T_{Mi,b}$ = temperature measured at the back PV/T module "i" (°C)
T_{PV} = temperature of PV cells (°)
T_{ST} = average temperature in the storage solar tank
$T_{ST,in}$ = water temperature at the inlet of storage solar tank (°C)
$T_{ST,out}$ = water temperature at the outlet of storage solar tank (°C)
$T_{ST,dw}$= water temperature in the lower part of storage solar tank (°C)
$T_{ST,up}$ = water temperature in the upper part of storage solar tank (°C)
Y_A = array yield (Wh/W)
Y_R = reference yield (Wh/W)

Greek symbols

β = tilt angle of the PV/T module (°)
γ = azimuth angle (°)
$\Delta T^{+}m$ = true mean fluid temperature difference (°C)
η = efficiency

Subscript

c=cooling
el = electrical
exp= experimental
i= index of PV/T modules [1, 2]
s=solar
sim = simulated
ST = solar tank
therm = thermal

Acronyms

DHW=domestic hot water
EL = electronic load
PR = Performance Ratio
QBTP=primary panel at low voltage
QBTS=secondary panel board at low voltage electrical board
SCADA = Supervisory Control and Data Acquisition
STC = Standard Test Condition

ACCEPTED MANUSCRIPT